

## Award Accounts

The Chemical Society of Japan Award for Young Chemists for 2006

# Development of Unique Chemical Phenomena within Nanometer-Sized, Self-Assembled Coordination Hosts

Michito Yoshizawa\*<sup>1,2</sup> and Makoto Fujita\*<sup>3</sup>

<sup>1</sup>Chemical Resources Laboratory, Tokyo Institute of Technology, 4259 Nagatsuta, Midori-ku, Yokohama 226-8503

<sup>2</sup>PRESTO, Japan Science and Technology Agency

<sup>3</sup>Department of Applied Chemistry, School of Engineering, The University of Tokyo, 7-3-1 Hongo, Bunkyo-ku, Tokyo 113-8656

Received February 10, 2010; E-mail: yoshizawa.m.ac@m.titech.ac.jp

This account recounts the application of self-assembled coordination hosts as molecular tools and the development of unusual chemical reactions and interactions generated within their cavities. Starting from the simple molecular recognition of guest molecules, coordination hosts have been used to accelerate reaction rates, endow regio- and stereoselectivity, and create unique reactions in their nanometer-sized cavities. Coordination hosts were also used to develop a new, practical method for constructing discrete stacks of aromatic molecules with unique electronic and magnetic properties.

## 1. Introduction

The local microenvironment has a large impact on the properties of molecules and within nanometer-sized cavities encapsulated molecules can exhibit unique behavior that cannot be observed or generated in bulk solution or the solid state.<sup>1</sup> Conventionally, the properties and reactivity of molecules are modulated and altered through the covalent introduction of substituent groups. More recently, the use of well-designed nanoscale cage molecules to impose specific, and occasionally unexpected, reaction pathways through non-covalent interactions has attracted considerable interest as an alternate pathway.<sup>1,2</sup> The behavior of guest molecules in nanometer-sized spaces were first studied in robust, solids, e.g., zeolites and mesoporous silica, and covalent host molecules, e.g., cyclodextrins, calixarenes, and carcerands. Over the last two decades the focus has shifted to harnessing non-covalent weak interactions and reversible bonds, hydrogen bonds and coordination bonds as respective examples, to construct cage frameworks hosting larger nanospaces.<sup>3,4</sup> The highly modular design and synthetic ease of constructing coordination hosts with functional cavities are particularly attractive and coordination hosts are now available in various sizes and shapes.<sup>5</sup>

At the beginning of this study, the properties and reactions of guest molecules in the cavities of coordination hosts were relatively unexplored.<sup>6</sup> In this account article, we would like to describe the development of unusual chemical properties, reactions, interactions, and phenomena that can occur in the nanometer-sized cavities of our self-assembled coordination hosts.

## 2. Molecular Recognition

In order to design new chemical reactions or generate unusual interactions, we must first understand the characteristics and properties of the host compounds. X-ray crystallography provides direct information about the size and shape of the cavity but the electronic and binding properties of molecular hosts must be examined through interactions with guest molecules. Our prototypical self-assembled coordination host **1**, used throughout this work, is prepared by simply mixing the tridentate triazine panel ligands and *cis*-protected Pd<sup>2+</sup> complexes in a 4:6 ratio (Figure 1).<sup>7</sup> In aqueous solution, organic molecules are driven into the hydrophobic cavity of water-soluble host **1** and the resultant clathrate complexes **1**⊃(guest)<sub>*n*</sub> (*n* = 1–4) are strongly bound via hydrophobicity, aromatic–aromatic interactions, and electrostatic interactions.<sup>8</sup>

**2.1 Molecular Ice.** Coordination host **1** is remarkably robust, and unlike many self-assembled molecular hosts that require an enclathrated guest to maintain integrity, exists in aqueous solution in the absence of any guest molecule. The question then arises: what is inside the hydrophobic cavity? And, if water molecules are located inside, how are they arranged? Water molecules are known to develop ordered hydrogen-bonded networks on the surface of hydrophobic substances, often giving rise to stable hydrate complexes.<sup>9</sup> We hypothesized that in the absence of guest molecules, water molecules would form an ordered endohedral network. X-ray crystallographic studies unambiguously revealed ten water molecules in an adamantane-like (H<sub>2</sub>O)<sub>10</sub> cluster within the

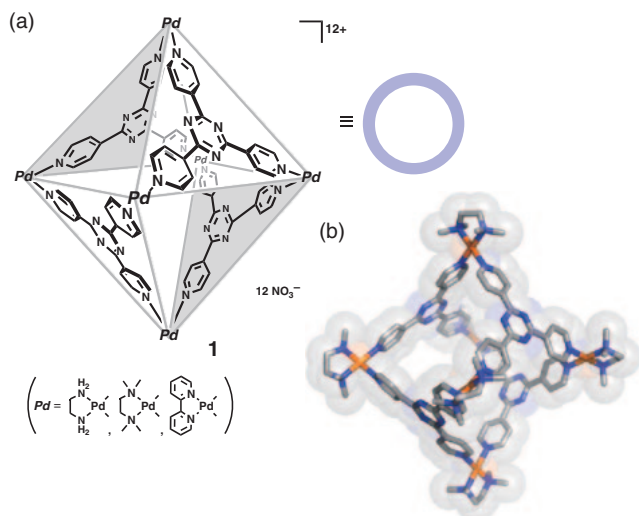


**Figure 1.** (a) Self-assembled coordination host **1** and (b) X-ray crystal structure of **1**.

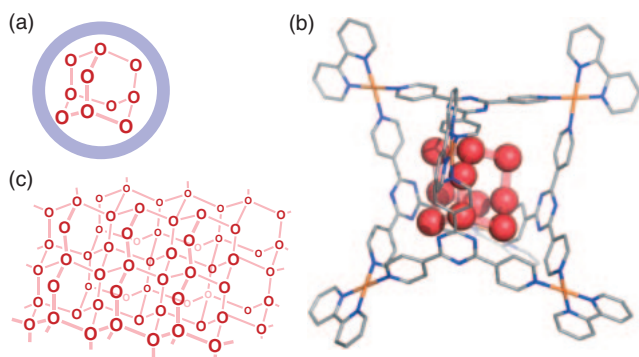


**Figure 2.** (a) Schematic representation and (b) X-ray crystal structure of a  $(\text{H}_2\text{O})_{10}$  cluster within host **1**. (c) Infinite network of water molecules in natural ice ( $I_c$ -type).

cavity of **1** (Figures 2a and 2b).<sup>10</sup> This arrangement is nearly identical to that of the smallest subunit of natural ice ( $I_c$ -type; Figure 2c) but the bridgehead is slightly compressed due to interactions with the four host panels. Neutron diffraction analysis located the deuterium nuclear density between the water oxygen atoms<sup>10</sup> and revealed that the lone pairs of the bridgehead oxygen atoms interact with the host panel  $\pi$ -systems; an unusual  $\text{H}_2\text{O}:\cdots\pi$  (lone pair– $\pi$  electron) interaction. As the structure of natural ice is defined as an infinite three-dimensional network of water molecules (Figure 2c), the finite  $(\text{H}_2\text{O})_{10}$  cluster in the cavity of **1** can be regarded as “molecular ice.”

**2.2 Bimolecular Recognition.** Molecular recognition in synthetic hosts has been extensively studied but the selective bimolecular recognition and encapsulation of two different guests in a single binding pocket remains non-trivial. Coordination host **1** however exhibits bimolecular recognition if the first guest is a large aromatic and the second an appropriately shaped aliphatic molecule.<sup>11</sup> For example, ternary host–guest complex **1**⊃(**2**·**3**) selectively formed in high yield (>90%) when perylene (**2**) and *cis*-decalin (**3**) (ca. 10-fold excess each) were suspended in an aqueous solution of **1** (Figure 3a). The

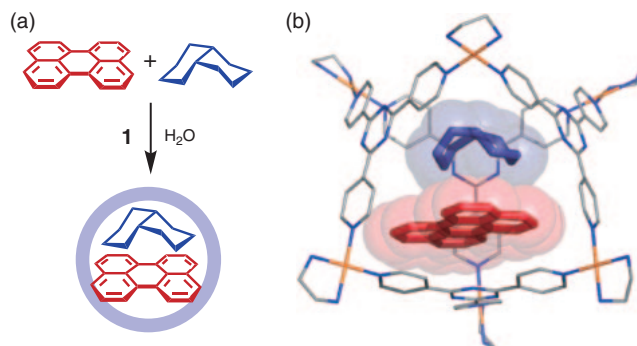


**Figure 3.** (a) Bimolecular recognition of two different guest molecules, perylene (**2**) and *cis*-decalin (**3**) within host **1**, and (b) optimized structure of **1**⊃(**2**·**3**).

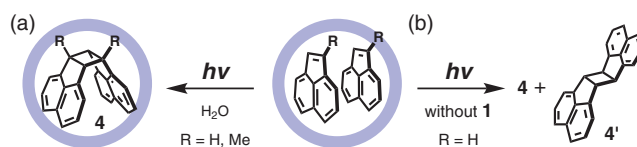


**Figure 4.** (a) Selective [2 + 2] photodimerization of acenaphthylenes within host **1** and (b) the photodimerization without **1**.

molecular modeling of the bimolecular inclusion complex revealed the importance of filling the hydrophobic space within host **1**; the aromatic perylene  $\pi$ -stacks on one panel ligand and the remaining void is filled by the bulky, aliphatic *cis*-decalin (Figure 3b). The combination of *cis*-decalin with pyrene, triphenylene, and coronene also afforded ternary inclusion complexes with host **1** despite the lack of specific recognition motifs or strong affinity between guest molecules. More recently, the diastereomeric bimolecular recognition of enantiomers was achieved within achiral coordination hosts.<sup>12</sup>

### 3. Chemical Reactions

The cavity of self-assembled host **1** is large enough to accommodate multiple guest molecules in water. Once entrapped, the confined environment of the host artificially raises the effective concentration and can force guest reactive sites into close proximity in specific and occasionally unusual orientations. As a result, remarkable enhancement of reaction rates and regio- and stereoselectivities can be produced within host **1**. In addition, interactions with the electron-deficient panels of host **1** results in unexpected reactions of enclathrated guest molecules.

**3.1 [2 + 2] Photodimerization.**<sup>13</sup> Self-assembled coordination hosts can be used as nanoscale “molecular flasks” to significantly accelerate photochemical reactions and control regio- and/or stereoselectivities. In 2002, the photoirradiation of an aqueous solution of coordination host **1** containing two acenaphthylene guest molecules selectively gave *syn*-dimer **4** ( $R = \text{H}$ ) in nearly quantitative yield (Figure 4a).<sup>14</sup> The reaction was easily monitored by  $^1\text{H}$ NMR analysis and product **4** was readily isolated by our standard extraction protocol from the final aqueous solution of **1**⊃**4**. In the absence of host **1**, significantly higher concentrations were required for the reaction to occur and *syn*-dimer **4** and *anti*-dimer **4'** were

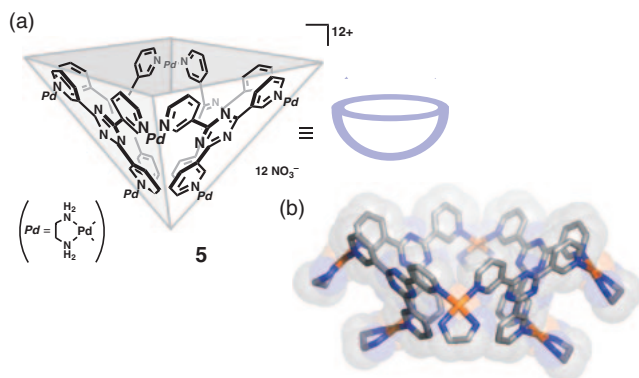


**Figure 5.** (a) Bowl-shaped coordination host **5** and (b) the X-ray crystal structure.

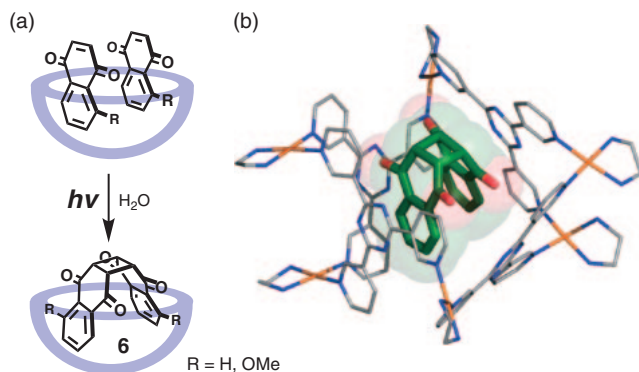


**Figure 6.** (a) Stereo- and regioselective [2 + 2] photodimerization of naphthoquinones within host **5** and (b) X-ray crystal structure of **5**⊃**6** (R = H).

obtained as a 1:1 mixture in low yield (Figure 4b). As an added side benefit, the aromatic panel framework of **1** filters all wavelengths shorter than ca. 310 nm, prevents the back reaction (dimer to monomer), and the reaction proceeds forward to near completion. 1-methylacenaphthylene is even less photoreactive, yet when two molecules were encapsulated, [2 + 2] photodimerization occurred and head-to-tail *syn*-dimer **4** (R = Me) was the exclusive product (Figure 4a).<sup>14,15</sup>

For the [2 + 2] photodimerization of naphthoquinones bowl-shaped coordination host **5**, with an open hydrophobic pocket (Figure 5),<sup>16</sup> gave *syn*-stereoisomer **6** in >98% yield (Figure 6a).<sup>14</sup> In the absence of host **5**, the reaction was slow even at high concentrations and the *anti*-photodimer was the main product (ca. 10:1 *anti*–*syn*). X-ray crystallographic analysis of encapsulated product **5**⊃**6** (R = H) revealed the snug fit between host **5** and the *syn*-product with several  $\pi$ – $\pi$  and CH– $\pi$  interactions (Figure 6b). The complementary shapes of molecular flask **5** and product **6** altered the reaction dynamics to favor the *syn*-stereoselectivity and head-to-tail regioselectivity. Even though the 5-position of naphthoquinone is remote from the reaction site, the photodimerization of 5-methoxy-1,4-naphthoquinone within **5** gave *syn* head-to-tail isomer **6** (R = OMe) in 80% yield (Figure 6a). Without host **5**, *anti*-isomers were obtained in low yield with no head-to-tail regioselectivity.

**3.2 Cross [2 + 2] Photodimerization.** Selective cross photodimerization is a particularly challenging subject in photochemistry as both substrates are of comparable reactivity.

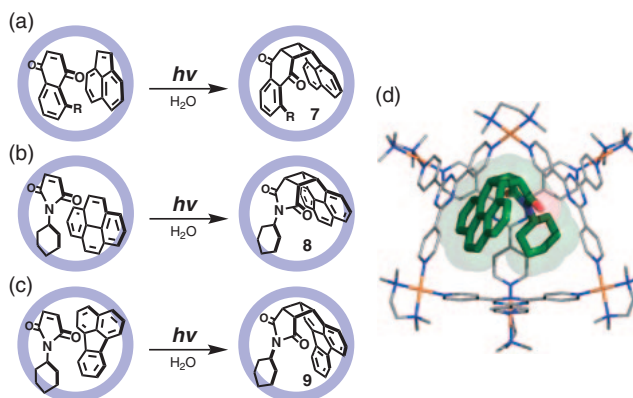


**Figure 7.** Cross [2 + 2] photodimerization of (a) 1,4-naphthoquinones and acenaphthylene, (b, c) *N*-cyclohexylmaleimide and pyrene or fluoranthene within host **1**. (d) X-ray crystal structure of **1**⊃**8**.

The photodimerization can be selectively accomplished when the two substrates are isolated in a molecular flask in a pairwise selective fashion. The heterodimer of acenaphthylene and 5-ethoxy-1,4-naphthoquinone was selectively entrapped when a 1:1 mixture was suspended in an aqueous solution of coordination host **1**, and after photoirradiation for 3 h hetero *syn*-photodimer **7** (R = OEt) was formed in ca. 90% yield (Figure 7).<sup>17</sup> The key factors essential for the cross photodimerization are co-encapsulation and pre-organization of the two substrates within the host framework and these are mainly regulated by steric bulk and shape. The bulky *N*-cyclohexylmaleimide is particularly well-suited for pairwise selective co-encapsulation and subsequent cross [2 + 2] photodimerization with planar arenes (e.g., acenaphthylene and dibenzosuberenone), selectively giving the *syn* hetero dimers in typically >90% yield.<sup>17</sup> Even inert arenes like pyrene, phenanthrene, or fluoranthene afforded the *syn* cross adducts (e.g., **8** and **9**) with the maleimides in the cavity of host **1** (Figures 7b–7d).<sup>18,19</sup> No cross-reactions occurred in the absence of **1**, even at high concentrations.

**3.3 Photoinduced Oxidation.** Molecular hosts are usually thought of as innocent bystanders that are only indirectly involved in the reaction pathways. However, self-assembled coordination host **1** is not only a simple vessel but can actively participate in the reactions of the entrapped substrates and produce new and unusual reactions. Independently, coordination host **1** and adamantane (**10**) are photochemically inert. However, the photoirradiation of 1:4 host–guest complex **1**⊃(**10**)<sub>4</sub> under aerobic conditions produced a mixture of oxidized adamantanes **11**, 1-adamantylhydroperoxide and 1-adamantanol, in 24% yield or in 96% yield assuming one guest is oxidized per host (Figure 8a).<sup>20</sup> X-ray crystallographic studies of **1**⊃(**10**)<sub>4</sub> revealed C–H... $\pi$  interactions between guest adamantanes and aromatic panels of **1** and detailed spectroscopic and theoretical analyses suggest that one of the four panels of **1** is first photochemically excited. Subsequent electron transfer from one encapsulated **10** gives a 1-adamantyl radical (plus H<sup>+</sup>) and the radical anion of **1**. The radical quickly reacts with O<sub>2</sub> and/or H<sub>2</sub>O and provides the oxidized products and regenerated **1**. The photoinduced radical anion of **1** was

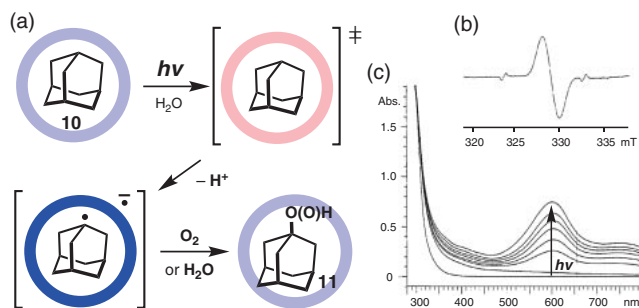


**Figure 8.** (a) Photoinduced oxidation of adamantane (**10**) within host **1**, (b) ESR spectrum of the photoinduced radical anion of **1**, and (c) UV-vis spectra of the photoirradiation of **1⊃(10)**<sub>4</sub>.

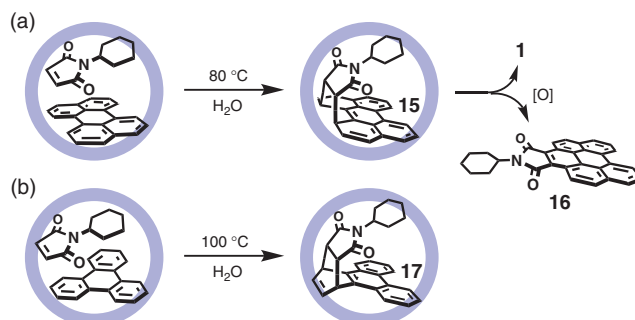


**Figure 10.** Diels-Alder reactions of typically inert (a) perylene and (b) triphenylene with maleimides within host **1**, respectively.

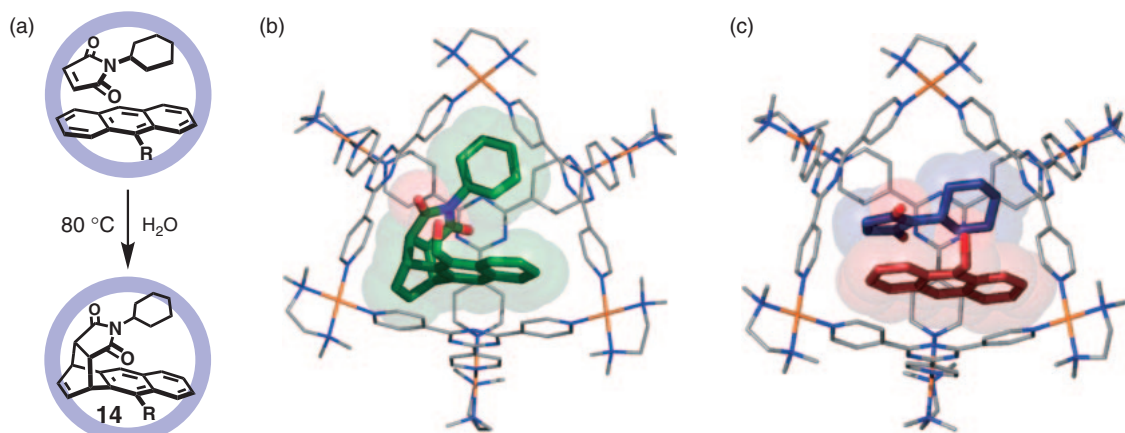


**Figure 9.** (a) Unusual Diels-Alder reaction of anthracenes and *N*-cyclohexylmaleimide within host **1**, (b) X-ray crystal structure of **1⊃14** (*R* = CH<sub>2</sub>OH), and (c) optimized structure of **1⊃(12·13)**.

clearly detected by ESR and UV-vis analyses under anaerobic conditions (Figures 8b and 8c). The reaction seems to be general and cyclic alkanes (e.g., cyclooctane) were also successfully photo-oxidized within host **1** to afford the corresponding alcohols and ketones.

**3.4 Diels-Alder Reactions.** Within self-assembled hosts, the rates of Diels-Alder reactions increase due to the enhanced effective molarity<sup>21</sup> and the guest pre-organization is expected to furnish unusual regio- and stereoselective Diels-Alder reactions. In 2006, we reported the Diels-Alder reaction of anthracene in coordination host **1**. Typically, dienophiles react at the central anthracene ring to give the 9,10-adduct, but in the cavity of host **1** *N*-cyclohexylmaleimide (**13**) reacted with the terminal rings of 9-hydroxymethylanthracene (**12**) to give *syn*-1,4-adduct **14** (*R* = CH<sub>2</sub>OH) in 98% yield (Figure 9a).<sup>22</sup> Carboxyl-, cyano-, and vinyl-substituted anthracenes all gave the 1,4-regioselective Diels-Alder products with *N*-cyclohexylmaleimide in high yields.<sup>22</sup> Selective bimolecular recognition of substrates **12** and **13** is essential for the reaction and was clearly observed by <sup>1</sup>H NMR analysis. Molecular modeling indicates that prior to the reaction the substrates are pre-organized with the olefin of **13** located close above the terminal ring of **12** and thus the 1,4-adduct is favored (Figure 9c). X-ray crystallographic analysis of host-product complex **1⊃14** (*R* = CH<sub>2</sub>OH) unambiguously revealed the structure of the *syn*-1,4-adduct (Figure 9b) and the tight fit and  $\pi$ -stacking

interactions (3.3 Å) between the aromatic rings of **14** and the host panels.

The limited cavity space within self-assembled hosts forces substrates into close proximity and can thus “activate” thermodynamically inert large arenes. Within host **1**, usually non-reactive perylene and *N*-cyclohexylmaleimide reacted to give *syn* Diels-Alder product **15** in 90% yield at 80 °C (Figure 10a).<sup>23</sup> Inside the protective framework of host **1**, **15** was stable and the structure of **15** was confirmed by the single-crystal X-ray diffraction of complex **1⊃15**. Once outside the host cavity however, **15** is rapidly oxidized in air to give compound **16** in less than 30 min. The Pt<sup>2+</sup>-analog of **1** is more robust and at 100 °C, highly inert triphenylene reacted with *N*-cyclohexylmaleimide to give Diels-Alder product **17** (Figure 10b).<sup>23</sup>

**3.5 Catalytic Diels-Alder Reactions.** Coordination hosts can be used to accelerate and alter chemical reactions, but typically in a stoichiometric fashion. Our ultimate goal is to engineer catalytic systems mimicking natural enzymes<sup>24</sup> and thus we used open coordination host **5** to catalyze the aqueous Diels-Alder reaction between maleimide and anthracene derivatives.<sup>22</sup> 10 mol % of bowl **5** sufficed to catalyze the Diels-Alder reaction between 9-hydroxymethylanthracene and *N*-phenylmaleimide yielding 9,10-adduct **18** (*R*<sub>1</sub> = CH<sub>2</sub>OH, *R*<sub>2</sub> = Ph) in quantitative yield after 5 h at room temperature (Figure 11). The reaction barely proceeded (3% yield) under



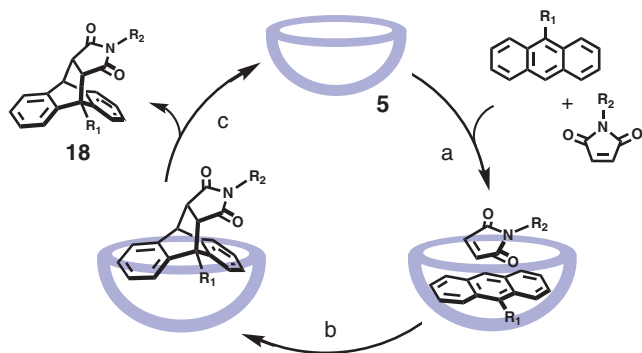


**Figure 11.** Catalytic Diels–Alder reaction of anthracene and maleimide derivatives in the presence of bowl-shaped coordination host **5** in water.

the same conditions in the absence of **5**. The most important steps in enzyme-like catalytic cycles are auto-inclusion and auto-exclusion.<sup>22</sup> First, the planar anthracene substrate enters the hydrophobic cavity and is bound by hydrophobic,  $\pi$ -stacking, and charge-transfer interactions (Figure 11a). The maleimide then fills the remaining space in the hydrophobic pocket and the reactive centers are held in close proximity. After the reaction, the anthracene moiety of product **18** is bent and can no longer efficiently  $\pi$ -stack with the host panel (Figure 11b). Accordingly, the weakly bound product is smoothly displaced by the incoming substrates and the catalytic cycle continues (Figure 11c). The catalysis mediates Diels–Alder reactions between a variety of anthracene and maleimide derivatives; i.e., 9-methyl-, 9-vinyl-, and 9-hydroxymethyl-anthracenes and *N*-propyl-, *N*-benzyl-, and *N*-phenylmaleimides.<sup>22</sup>

**3.6 Sol–Gel Condensation.** The isolation and characterization of reactive species during polymerization is a challenging subject due to the mixture of short-lived reactive intermediates.<sup>25</sup> In 2000, we reported that coordination host **1** could trap and stabilize short-lived, cyclic silanol trimers **19** formed during the sol–gel condensation of trialkoxysilanes. CSI-MS and NMR spectrometries revealed that cyclic trimer **19** ( $R = H$ ) was selectively prepared and sequestered when phenyltrimethoxysilane polymerized in an aqueous solution of host **1** (Figure 12a).<sup>26</sup> More importantly, clathrate complex **1**⊃**19** was isolated in >90% yield as a pure solid. Final structural proof was provided by X-ray crystallographic analysis and the all-*cis* conformation of the cyclic trimer was revealed (Figure 12b).<sup>27</sup> The three highly reactive Si–OH groups of **19** are fully protected by the host framework, suppressing further condensation and the typically elusive trimer is stable even in acidic aqueous solutions. Similar to the construction of a “ship-in-a-bottle,” the substrates are small enough to freely enter and exit host **1**, but once formed product **19** is too large and can no longer escape.

Judicious choice of host cavity allowed the selective isolation of specific silanol intermediates. When 2-naphthyl-trimethoxysilane (**20**) polymerized in an aqueous solution of bowl-shaped host **5**, silanol dimer **21** was sequestered and isolated in ca. 90% yield (Figure 13a).<sup>27</sup> Tube-shaped host **22**<sup>28</sup> could only encapsulate one molecule of **20** which was then hydrolyzed to give trisilanol **23** in high yield.<sup>27</sup> These

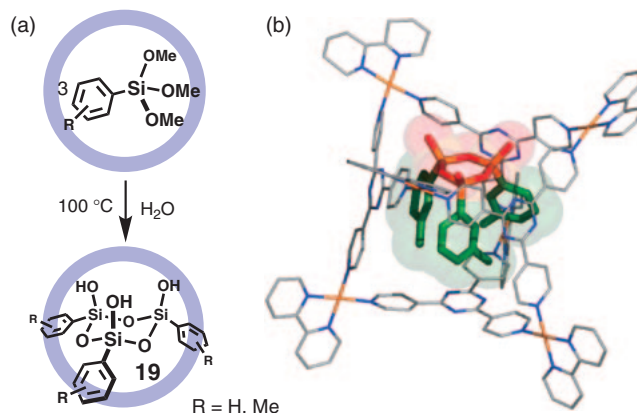


**Figure 12.** (a) Sol–gel condensation of trialkoxysilanes into cyclic trimers **19** within host **1** and (b) X-ray crystal structure of **1**⊃**19** ( $R = Me$ ).

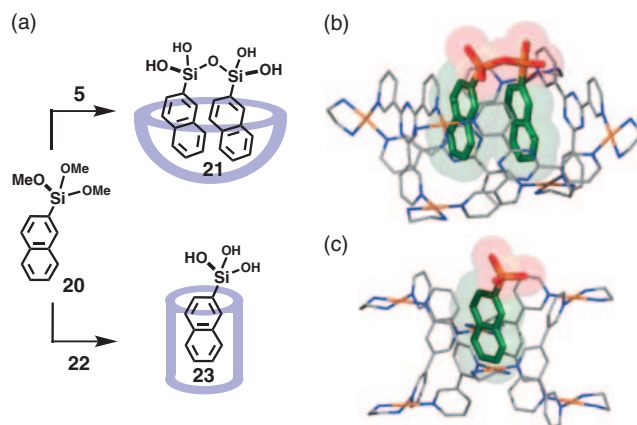


**Figure 13.** (a) Isolation of reactive species in the polycondensation of trialkoxysilanes within coordination hosts **5** and **22** in water and X-ray crystal structures of (b) **5**⊃**21** and (c) **22**⊃**23**.

intermediates are fleetingly ephemeral species during the sol–gel condensation, due to the highly reactive Si–OH groups, but are stable, isolable, and easily characterized by NMR, MS, and X-ray crystallographic analyses (Figures 13b and 13c).

#### 4. Molecular Stacks

Discrete stacks of aromatic molecules with specific heights and order are of great importance to the fields of  $\pi$ -conjugated functional materials.<sup>29</sup> In a novel approach, we used self-assembled coordination hosts as molecular templates to construct finite aromatic stacks and avoid lengthy covalent syntheses. In 2005, we designed prism-shaped coordination host **24** with a cavity capable of accommodating two planar aromatics in a stacked fashion.<sup>30</sup> Coordination host **24** selectively assembled from three pillar and two panel ligands in the presence of templating aromatic molecules (Figure 14a). Two aromatic molecules, such as pyrene, triphenylene, and coronene, form  $\pi$ -stacked dimers within host **24** through  $\pi$ -stacking and hydrophobic host–guest interactions (Figure 14b). The cavity height and the number of stacked guests can be increased by simply changing the length of the pillar ligand (Figure 14c).<sup>30</sup>

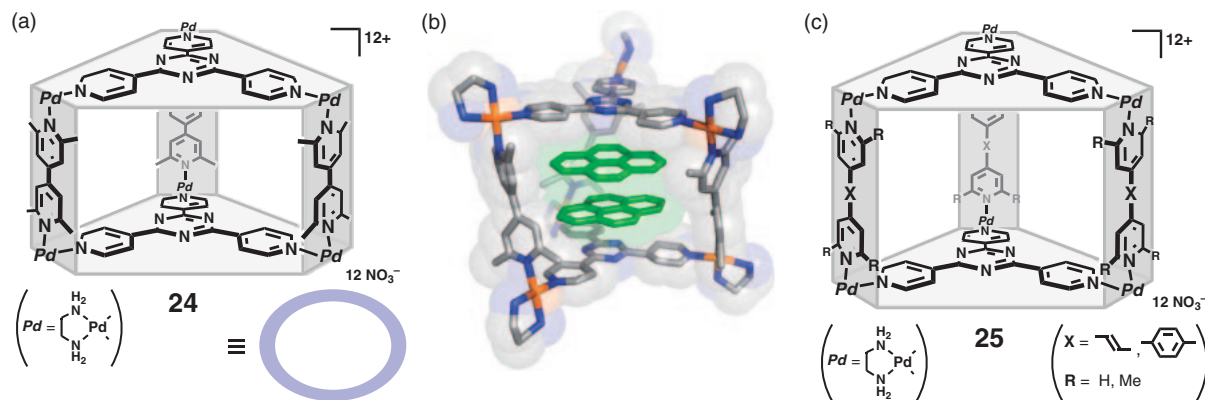


**Figure 14.** (a) Prism-shaped coordination host **24**, (b) X-ray crystal structure of **24** with two molecules of pyrene, and (c) the derivatives of prism-shaped host (**25**).

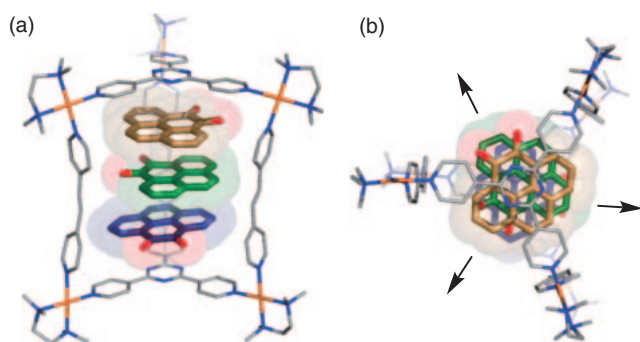


**Figure 15.** X-ray crystal structure of triple stacked, polarized aromatic molecules **26** within host **25**. (a) Side and (b) top views.

**4.1 Polarized Aromatic Molecule.** Dipole–dipole interactions between molecules are relatively weak but important attractive forces. In the solid state, polarized aromatic molecules such as pyrene-4,5-dione (**26**; 6.1–6.7 D) form infinite, head-to-tail columnar stacks that effectively cancel the net dipole.<sup>31</sup> If an odd number of **26** stacks, however, a head-to-tail stacked conformation cannot cancel the net dipole moment. Host–guest complex **25**⊃(**26**)<sub>3</sub> contains three stacked polarized aromatics and quantitatively assembled when pyrenedione **26** was mixed with the components of host **25** in aqueous solution.<sup>32</sup> X-ray crystallographic analysis revealed that the three guest molecules do not stack in a head-to-tail fashion but are rotated by 120° with respect to each other (Figure 15). By systematically altering the cavity height, discrete stacks of two, three, four, and five polarized aromatic **26** were constructed in a selective fashion.<sup>32</sup>

**4.2 The Mixed-Valence State of TTF.** The electrochemical properties of tetrathiafulvalene (TTF; **27**) within molecular hosts have been exhaustively examined but when trapped within host **24**, an unusual mixed-valence state of stacked tetrathiafulvalene dimer [(**27**)<sub>2</sub>]<sup>•+</sup> was generated at room temperature in aqueous solution. When excess **27** was added to an aqueous solution of **24**, the colorless solution quickly turned dark green as **24**⊃(**27**)<sub>2</sub> complex formed (Figure 16a).<sup>33</sup> Electrochemical studies revealed that an initial one-electron oxidation occurs at ca. 150 mV giving mixed-valence dimer

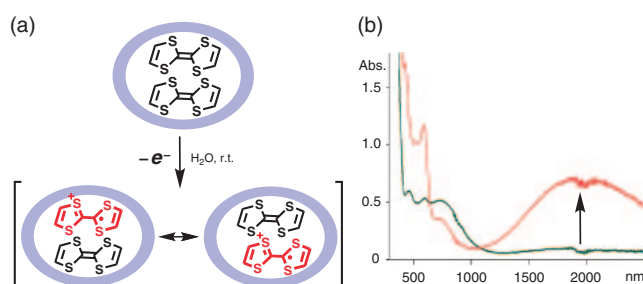


**Figure 16.** (a) Stable formation of the mixed-valence state of TTF dimer within prism-shaped host **24** and (b) UV-vis spectra of **24**⊃(**27**)<sub>2</sub> and **24**⊃[(**27**)<sub>2</sub>]<sup>•+</sup>.

[(**27**)<sub>2</sub>]<sup>•+</sup> and a second one-electron oxidation at ca. 300 mV gives cation radical dimer (**27**<sup>•+</sup>)<sub>2</sub>. The mixed-valence state was also indicated by the appearance of a broad absorption band in the near-infrared region ( $\lambda_{\text{max}} \approx 2000$  nm) of the UV-vis spectrum of **24**⊃(**27**)<sub>2</sub> at a constant voltage of 180 mV (Figure 16b). The host framework forces the two molecules of **27** into close proximity, and protected within the host framework, the mixed-valence dimer is protected from oxygen and solvent molecules and is unusually stable, even at room temperature and in aqueous solution ( $t_{1/2} \approx 1$  day).

**4.3 Stack of Metal-Complexes.** We next exploited the stacked conformation of planar metal complexes within host **24** to generate specific metal–metal interactions. The strict control of the spatial arrangement of metal ions and their interactions is of considerable interest for the development of molecular-based electronic and magnetic materials. Bisacetylacetonato metal-complexes (**28**<sub>M</sub>) are classic, well-known planar compounds but intermolecular metal–metal interactions had not yet been observed. Upon addition of **28**<sub>M</sub> (M = Pt<sup>2+</sup>, Pd<sup>2+</sup>, and Cu<sup>2+</sup>) to an aqueous solution of **24**, two molecules of complexes **28**<sub>M</sub> entered the cavity and formed stable stacked dimers (Figure 17a).<sup>34</sup> X-ray crystallographic analysis of host–guest complex **24**⊃(**28**<sub>Pt</sub>)<sub>2</sub> revealed the Pt atoms in close contact, ca. 3.3 Å (Figure 17b); Typical metal–metal d–d interactions are 3.1–3.5 Å. The metal–metal d–d interactions were also apparent in the UV-vis spectra of **24**⊃(**28**<sub>M</sub>)<sub>2</sub> as broad absorptions (around 450 nm when M = Pt<sup>2+</sup> and 500 nm when M = Pd<sup>2+</sup>). Spin–spin exchange interactions between two Cu<sup>2+</sup> centers were observed for complex **24**⊃(**28**<sub>Cu</sub>)<sub>2</sub>.

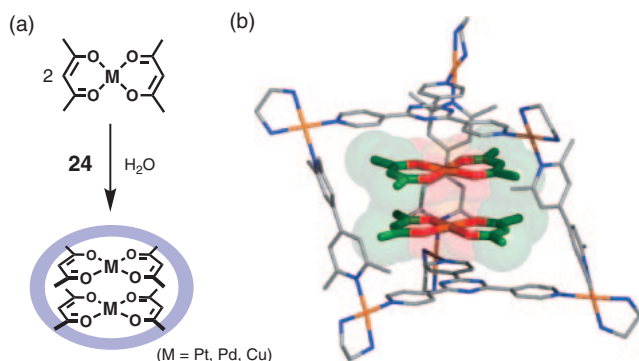


**Figure 17.** (a) Metal–metal d–d interactions through the stack of two metal–complexes  $28_M$  ( $M = \text{Pt}^{2+}$ ,  $\text{Pd}^{2+}$ , and  $\text{Cu}^{2+}$ ) within host  $24$  and (b) X-ray crystal structure of  $24 \supset (28_{\text{Pt}})_2$ .

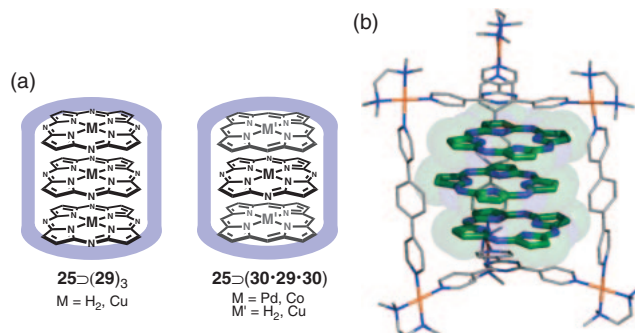


**Figure 18.** (a) Homo and hetero triple stacks of metal–azaporphine ( $29$ ) and metal–porphine ( $30$ ) within prism-shaped host  $25$  and (b) X-ray crystal structure of  $25 \supset (29)_3$  ( $M = \text{H}_2$ ).

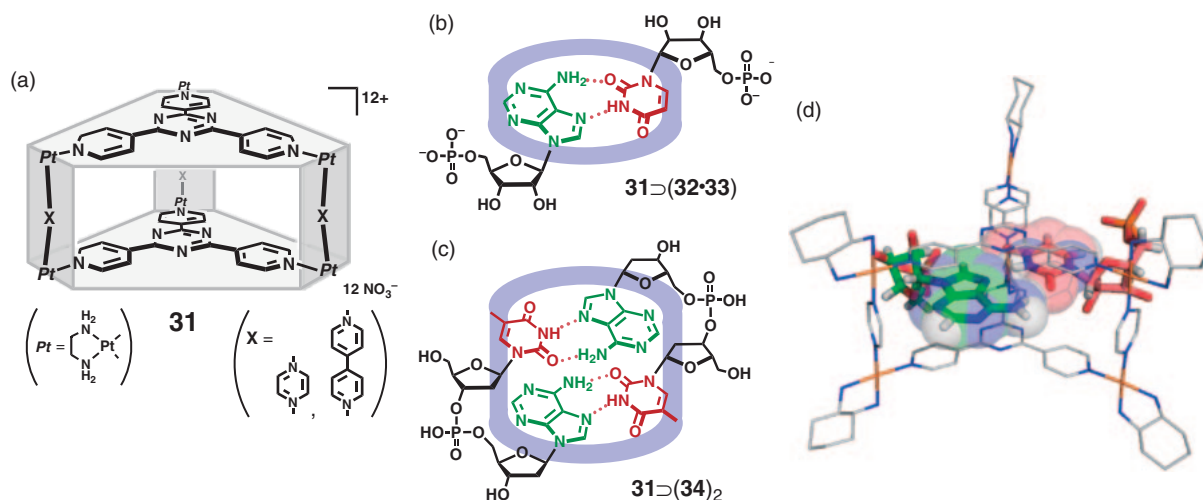


**Figure 19.** (a) Coordination hosts  $31$  with robust platinum(II) complexes, stabilization of hydrogen-bonding pairs of (b) mononucleotides  $32$  and  $33$  and (c) dinucleotides  $34$  within host  $31$ , and (d) X-ray crystal structure of  $31 \supset (32 \cdot 33)$ .

Inserting a phenylene spacer into the pillar-like ligand led to extended prism-shaped host  $25$  ( $X = -\text{C}_6\text{H}_4-$ ,  $R = \text{CH}_3$ ) suitable for accommodating triple stacks of aromatic guests and a three metal  $\text{Cu}^{2+}$ – $\text{Cu}^{2+}$ – $\text{Cu}^{2+}$  array was obtained when  $\text{Cu}^{2+}$ -containing azaporphine molecules were encapsulated (Figure 18).<sup>35</sup> Exciton couplings between the stacked guests were observed in the UV–vis spectrum and ESR analysis revealed a ferromagnetically coupled quartet state ( $S = 3/2$ ) for the three  $\text{Cu}^{2+}$  centers. The  $\Delta m_s = 3$  forbidden transition was observed at a field strength of 100 mT and is the first report for an inorganic system. Alternating donor–acceptor–donor stacks are favored due to electrostatic interactions and when electron-deficient azaporphine ( $29$ ) and electron-rich porphine ( $30$ ) were added to the components of host  $25$ , alternating complex  $25 \supset (30 \cdot 29 \cdot 30)$  was generated. Alternating mixed metal triple stacks were then prepared using porphine and azaporphine metal complexes (where  $M = \text{Pd}^{2+}$ ,  $\text{Co}^{2+}$  and  $M' = \text{Cu}^{2+}$ ,  $\text{H}_2$ ) (Figure 18a). ESR studies demonstrated that the two  $\text{Cu}^{2+}$  centers interact through the  $\text{Co}^{2+}$  center, but the  $\text{Pd}^{2+}$  center suppresses spin–spin exchange.<sup>35</sup> Enclathration of a planar  $\text{Ni}^{2+}$ -complex within host  $24$  was recently shown to induce

spin-crossover behavior without changing the coordination number and geometry.<sup>36,37</sup>

**4.4 Nucleotide Stack.** Mono- and dinucleotide fragments are unable to form stable hydrogen-bonded base pairs or duplexes in water, but in the hydrophobic pockets of enzymes and proteins however, even short fragments can form stable duplexes to transmit genetic information. We recently demonstrated that the artificial hydrophobic cavity of platinum host  $31$  can also stabilize and isolate minimal base pairs in aqueous solution (Figures 19a–19c).<sup>38</sup> Simply mixing 5'-adenosine monophosphate ( $32$ ) and 5'-uridine monophosphate ( $33$ ) in an aqueous solution of  $31$  ( $X = 1,4$ -pyridine) gave host–guest complex  $31 \supset (32 \cdot 33)$ . X-ray crystallographic analysis of the complex clearly revealed the selective formation of a Hoogsteen hydrogen-bonded base pair for  $32$  and  $33$  (Figure 19d). When  $X = 4,4'$ -bipyridine, the dinucleotide thymidylyl-(3'-5')-2'-deoxyadenosine ( $34$ ) formed a stable stacked Hoogsteen base pair duplex inside host  $31$  in water (Figure 19c).

**4.5 Interlocked Aromatic Stacks.** Inspired by the aromatic stacks buried within catenanes,<sup>39</sup> we hypothesized that interlocked molecular hosts would provide a framework for



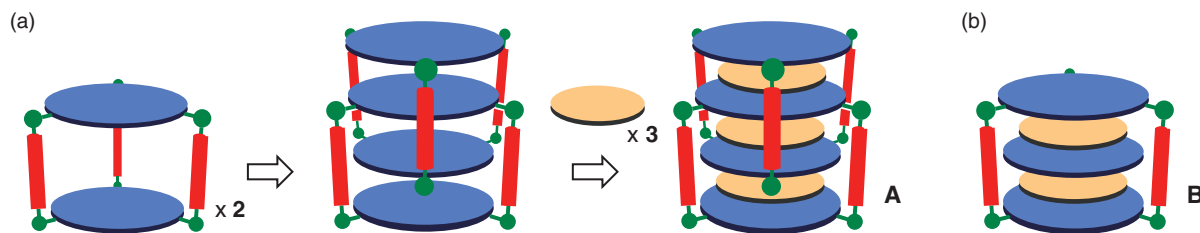


**Figure 20.** (a) The hypothesized construction of extended aromatic stack via interlocked coordination cages. The interlocked cages define three voids where aromatic guest molecules can intercalate and generate an alternating D–A aromatic stack. (b) A stable intermediate is most likely formed first during self-assembly.

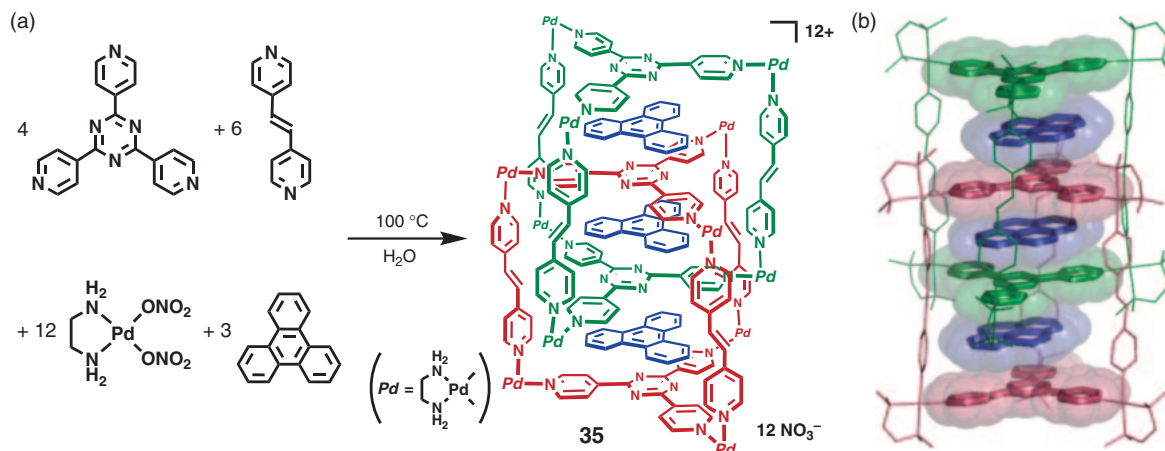


**Figure 21.** (a) Schematic representation of the preparation of septuple aromatic stack **35** and (b) X-ray crystal structure of **35** (aromatic molecules: pyrene).

constructing extended stacked aromatic molecules **A** in discrete manner (Figure 20a). When the appropriate pillar ligands, panel ligands, triphenylene template, and end-capped  $\text{Pd}^{2+}$  complex (in a 6:4:3:12 ratio) were suspended in water and stirred at 100 °C, septuple aromatic stack **35** was obtained in almost quantitative yield (Figure 21a).<sup>40</sup> In the  $^1\text{H}$ NMR spectrum two intercalated triphenylene guest signals were observed in a 2:1 ratio and both sets were considerably shifted upfield due to shielding by the triazine panel ligands. CSI-MS spectrometry also confirmed the expected molecular mass of this unique structure and X-ray crystallography unequivocally provided the final evidence. The 2.1 nm long aromatic column of **35** is formed through efficient aromatic–aromatic interaction between all seven aromatic subunits (3.3 Å between adjacent molecules) (Figure 21b). In hindsight, our hypothesis was slightly misleading as stable intermediate **B** (Figure 20b) is most likely formed first during self-assembly and the second, interlocked coordination cage locks into place afterwards.

This method is highly effective and was successfully applied to the construction of even taller discrete stacks. Using molecular modeling, we carefully designed elongated pillar ligands **36** and **37**, and when combined with the correct ratio of triazine panels, metal ions, and pyrene guests, octuple stack **38** and nonuple stack **39** respectively assembled in almost quantitative yields (Figure 22).<sup>40</sup> The X-ray crystal structure of **38** confirmed the 2.4 nm tall cylindrical stack of aromatic molecules and the even larger **39** was calculated to be 2.7 nm tall (Figures 22b and 22c). These nanometer-sized aromatic towers provide well-defined systems in between simple dimers

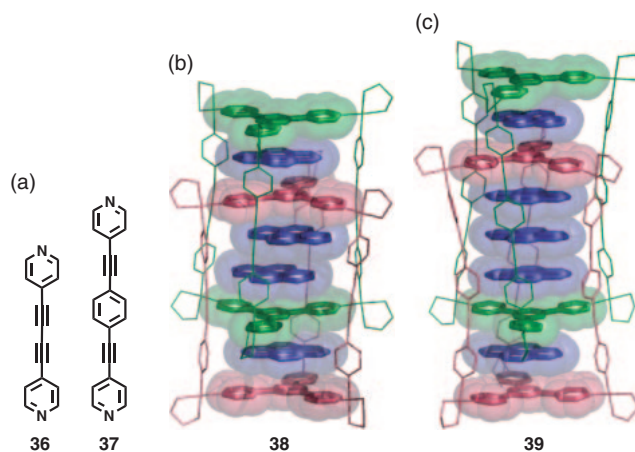


**Figure 22.** (a) Organic pillars **36** and **37**, (b) X-ray crystal structure of octuple stack **38**, and (c) optimized structure of nonuple stack **39**.

and infinite stacks where the extent of transannular conjugation can be controlled and are of great interest as potential elements for the nanofabrication of electroconductive and photophysical devices.

## 5. Conclusion

In this account, we have described our recent undertaking to develop and establish self-assembled coordination hosts as molecular tools for engineering new and unusual chemical



reactions and interactions. Starting with the simple molecular recognition of guest molecules, we applied coordination hosts to not only accelerate reaction rates and endow regio- and stereoselectivity but also to create unique reactions. Just as one selects appropriate glassware for a reaction scale, we have shown that size and shape of the nanometer-sized molecular flasks are just as important in controlling reactions on a molecular level. Unlike conventional synthetic chemistry, we can use our self-assembled molecular hosts to directly control and alter chemical reactions without covalently modifying the substrates. We have also applied coordination hosts to generate new and unusual interactions between guest molecules and developed a useful method for making discrete stacks of aromatic molecules with unique electronic and magnetic properties. The size and shape of the molecular container is tunable and precisely regulates the number and order of stacked molecules in turn. These simple yet powerful tools will open the doorway for the design of novel green reactions and the engineering of unique molecular elements for functional devices and materials. We believe that the possibilities inside the nanometer cavities of finite coordination hosts are infinite.

We would like to express our sincere appreciation to all the co-workers for their efforts and cooperation, whose names are cited in the references. This project has been supported in part by a grant from the Ministry of Education, Culture, Sports, Science and Technology of Japan (Nos. 20750042 and area 2107).

## References

- 1 a) D. J. Cram, J. M. Cram, *Container Molecules and Their Guests*, Royal Society of Chemistry, Cambridge, **1994**. b) J. W. Steed, J. L. Atwood, *Supramolecular Chemistry*, 1st ed., Wiley, Chichester, **2000**.
- 2 D. M. Vriezema, M. C. Aragonès, J. A. A. W. Elemans, J. J. L. M. Cornelissen, A. E. Rowan, R. J. M. Nolte, *Chem. Rev.* **2005**, *105*, 1445.
- 3 L. R. MacGillivray, J. L. Atwood, *Angew. Chem., Int. Ed.* **1999**, *38*, 1018.
- 4 a) F. Hof, S. L. Craig, C. Nuckolls, J. Rebek, Jr., *Angew. Chem., Int. Ed.* **2002**, *41*, 1488. b) J. Rebek, *Angew. Chem., Int. Ed.* **2005**, *44*, 2068.
- 5 a) D. L. Caulder, K. N. Raymond, *Acc. Chem. Res.* **1999**, *32*, 975. b) S. Leininger, B. Olenyuk, P. J. Stang, *Chem. Rev.* **2000**, *100*, 853. c) M. Fujita, M. Tominaga, A. Hori, B. Therrien, *Acc. Chem. Res.* **2005**, *38*, 369.
- 6 a) D. Fiedler, D. H. Leung, R. G. Bergman, K. N. Raymond, *Acc. Chem. Res.* **2005**, *38*, 349. b) C. H. M. Amijs, G. P. M. van Klink, G. van Koten, *Dalton Trans.* **2006**, 308. c) M. Yoshizawa, J. K. Klosterman, M. Fujita, *Angew. Chem., Int. Ed.* **2009**, *48*, 3418.
- 7 M. Fujita, D. Oguro, M. Miyazawa, H. Oka, K. Yamaguchi, K. Ogura, *Nature* **1995**, *378*, 469.
- 8 a) T. Kusukawa, M. Fujita, *Angew. Chem., Int. Ed.* **1998**, *37*, 3142. b) F. Ibukuro, T. Kusukawa, M. Fujita, *J. Am. Chem. Soc.* **1998**, *120*, 8561. c) T. Kusukawa, M. Fujita, *J. Am. Chem. Soc.* **1999**, *121*, 1397. d) T. Kusukawa, M. Yoshizawa, M. Fujita, *Angew. Chem., Int. Ed.* **2001**, *40*, 1879. e) T. Kusukawa, M. Fujita, *J. Am. Chem. Soc.* **2002**, *124*, 13576.
- 9 a) D. Eisenberg, W. Kauzmann, *The Structure and Properties of Water*, Oxford University Press, New York, **1969**. b) F. H. Stillinger, *Science* **1980**, *209*, 451. c) R. Ludwig, *Angew. Chem., Int. Ed.* **2001**, *40*, 1808.
- 10 M. Yoshizawa, T. Kusukawa, M. Kawano, T. Ohhara, I. Tanaka, K. Kurihara, N. Niimura, M. Fujita, *J. Am. Chem. Soc.* **2005**, *127*, 2798.
- 11 M. Yoshizawa, M. Tamura, M. Fujita, *J. Am. Chem. Soc.* **2004**, *126*, 6846.
- 12 M. Yoshizawa, M. Tamura, M. Fujita, *Angew. Chem., Int. Ed.* **2007**, *46*, 3874.
- 13 a) N. J. Turro, G. S. Cox, M. A. Paczkowski, *Top. Curr. Chem.* **1985**, *129*, 57. b) V. Ramamurthy, K. Venkatesan, *Chem. Rev.* **1987**, *87*, 433. c) V. Ramamurthy, D. Eaton, *Acc. Chem. Res.* **1988**, *21*, 300. d) *Solid State and Surface Photochemistry. Molecular and Supramolecular Photochemistry*, ed. by V. Ramamurthy, K. S. Schanze, Marcel Dekker, New York, **2000**, Vol. 5. e) R. S. Liu, G. S. Hammond, *Acc. Chem. Res.* **2005**, *38*, 396. f) M. N. Chrétien, *Pure Appl. Chem.* **2007**, *79*, 1.
- 14 M. Yoshizawa, Y. Takeyama, T. Kusukawa, M. Fujita, *Angew. Chem., Int. Ed.* **2002**, *41*, 1347.
- 15 Related works: a) S. Karthikeyan, V. Ramamurthy, *Tetrahedron Lett.* **2005**, *46*, 4495. b) K. Takaoka, M. Kawano, T. Ozeki, M. Fujita, *Chem. Commun.* **2006**, 1625. c) L. S. Kaanumalle, V. Ramamurthy, *Chem. Commun.* **2007**, 1062.
- 16 a) M. Fujita, S.-Y. Yu, T. Kusukawa, H. Funaki, K. Ogura, K. Yamaguchi, *Angew. Chem., Int. Ed.* **1998**, *37*, 2082. b) S.-Y. Yu, T. Kusukawa, K. Biradha, M. Fujita, *J. Am. Chem. Soc.* **2000**, *122*, 2665.
- 17 M. Yoshizawa, Y. Takeyama, T. Okano, M. Fujita, *J. Am. Chem. Soc.* **2003**, *125*, 3243.
- 18 Y. Nishioka, T. Yamaguchi, M. Yoshizawa, M. Fujita, *J. Am. Chem. Soc.* **2007**, *129*, 7000.
- 19 Related works: a) T. Furusawa, M. Kawano, M. Fujita, *Angew. Chem., Int. Ed.* **2007**, *46*, 5717. b) T. Yamaguchi, M. Fujita, *Angew. Chem., Int. Ed.* **2008**, *47*, 2067. c) Y. Nishioka, T. Yamaguchi, M. Kawano, M. Fujita, *J. Am. Chem. Soc.* **2008**, *130*, 8160.
- 20 a) M. Yoshizawa, S. Miyagi, M. Kawano, K. Ishiguro, M. Fujita, *J. Am. Chem. Soc.* **2004**, *126*, 9172. b) Y. Furutani, H. Kandori, M. Kawano, K. Nakabayashi, M. Yoshizawa, M. Fujita, *J. Am. Chem. Soc.* **2009**, *131*, 4764.
- 21 a) J. Kang, J. Rebek, Jr., *Nature* **1997**, *385*, 50. b) T. Kusukawa, T. Nakai, T. Okano, M. Fujita, *Chem. Lett.* **2003**, *32*, 284.
- 22 M. Yoshizawa, M. Tamura, M. Fujita, *Science* **2006**, *312*, 251.
- 23 Y. Nishioka, T. Yamaguchi, M. Yoshizawa, M. Fujita, *J. Am. Chem. Soc.* **2007**, *129*, 7000.
- 24 a) J. Kang, J. Santamaría, G. Hilmersson, J. Rebek, Jr., *J. Am. Chem. Soc.* **1998**, *120*, 7389. b) H. Ito, T. Kusukawa, M. Fujita, *Chem. Lett.* **2000**, 598. c) M. Yoshizawa, N. Sato, M. Fujita, *Chem. Lett.* **2005**, *34*, 1392. d) D. Fiedler, R. G. Bergman, K. N. Raymond, *Angew. Chem., Int. Ed.* **2004**, *43*, 6748. e) M. D. Pluth, R. G. Bergman, K. N. Raymond, *Science* **2007**, *316*, 85. f) M. L. Merlau, M. del Pilar Mejia, S. T. Nguyen, J. T. Hupp, *Angew. Chem., Int. Ed.* **2001**, *40*, 4239. g) S. J. Lee, S.-H. Cho, K. L. Mulfort, D. M. Tiede, J. T. Hupp, S. T. Nguyen, *J. Am. Chem. Soc.* **2008**, *130*, 16828.
- 25 a) M. Ziegler, J. L. Brumaghim, K. N. Raymond, *Angew. Chem., Int. Ed.* **2000**, *39*, 4119. b) M. Kawano, Y. Kobayashi, T. Ozeki, M. Fujita, *J. Am. Chem. Soc.* **2006**, *128*, 6558. c) V. M. Dong, D. Fiedler, B. Carl, R. G. Bergman, K. N. Raymond, *J. Am.*

*Chem. Soc.* **2006**, 128, 14464. d) T. Iwasawa, R. J. Hooley, J. Rebek, Jr., *Science* **2007**, 317, 493. e) P. Mal, B. Breiner, K. Rissanen, J. R. Nitschke, *Science* **2009**, 324, 1697.

26 M. Yoshizawa, T. Kusukawa, M. Fujita, K. Yamaguchi, *J. Am. Chem. Soc.* **2000**, 122, 6311.

27 M. Yoshizawa, T. Kusukawa, M. Fujita, S. Sakamoto, K. Yamaguchi, *J. Am. Chem. Soc.* **2001**, 123, 10454.

28 M. Aoyagi, K. Biradha, M. Fujita, *J. Am. Chem. Soc.* **1999**, 121, 7457.

29 a) C. A. Hunter, *Chem. Soc. Rev.* **1994**, 23, 101. b) C. A. Hunter, K. R. Lawson, J. Perkins, C. J. Urch, *J. Chem. Soc., Perkin Trans. 2* **2001**, 651. c) R. J. Bushby, O. R. Lozman, *Curr. Opin. Colloid Interface Sci.* **2002**, 7, 343. d) J. K. Klosterman, Y. Yamauchi, M. Fujita, *Chem. Soc. Rev.* **2009**, 38, 1714.

30 a) M. Yoshizawa, J. Nakagawa, K. Kumazawa, M. Nagao, M. Kawano, T. Ozeki, M. Fujita, *Angew. Chem., Int. Ed.* **2005**, 44, 1810. b) M. Yoshizawa, M. Nagao, K. Kumazawa, M. Fujita, *J. Organomet. Chem.* **2005**, 690, 5383.

31 Z. Wang, V. Enkelmann, F. Negri, K. Müllen, *Angew. Chem., Int. Ed.* **2004**, 43, 1972.

32 a) Y. Yamauchi, M. Yoshizawa, M. Akita, M. Fujita, *Proc. Natl. Acad. Sci. U.S.A.* **2009**, 106, 10435. b) Y. Yamauchi, M. Yoshizawa, M. Akita, M. Fujita, *J. Am. Chem. Soc.* **2010**, 132, 960.

33 M. Yoshizawa, K. Kumazawa, M. Fujita, *J. Am. Chem. Soc.* **2005**, 127, 13456.

34 M. Yoshizawa, K. Ono, K. Kumazawa, T. Kato, M. Fujita, *J. Am. Chem. Soc.* **2005**, 127, 10800.

35 a) K. Ono, M. Yoshizawa, T. Kato, K. Watanabe, M. Fujita, *Angew. Chem., Int. Ed.* **2007**, 46, 1803. b) K. Ono, M. Yoshizawa, T. Kato, M. Fujita, *Chem. Commun.* **2008**, 2328.

36 K. Ono, M. Yoshizawa, M. Akita, T. Kato, Y. Tsunobuchi, S. Ohkoshi, M. Fujita, *J. Am. Chem. Soc.* **2009**, 131, 2782.

37 K. Ono, J. K. Klosterman, M. Yoshizawa, K. Sekiguchi, T. Tahara, M. Fujita, *J. Am. Chem. Soc.* **2009**, 131, 12526.

38 T. Sawada, M. Yoshizawa, S. Sato, M. Fujita, *Nat. Chem.* **2009**, 1, 53.

39 M. Fujita, *Acc. Chem. Res.* **1999**, 32, 53.

40 Y. Yamauchi, M. Yoshizawa, M. Fujita, *J. Am. Chem. Soc.* **2008**, 130, 5832.



Award recipient

Michito Yoshizawa received his B.S. from Tokyo University of Agriculture and Technology in 1997, M.S. from Tokyo Institute of Technology in 1999, and then Ph.D. from Nagoya University in 2002 under Prof. Makoto Fujita. He moved to The University of Tokyo with Prof. Fujita as a JSPS postdoctoral fellow and became Assistant Professor in 2003. He has been a researcher of the PRESTO (Precursory Research for Embryonic Science and Technology) project of Japan Science and Technology Agency (JST) since 2006. In 2008, he became Associate Professor at the Chemical Resources Laboratory, Tokyo Institute of Technology. His current research interests focus on molecular recognition as well as chemical reactions and properties within supramolecular complexes.



Makoto Fujita received his Ph.D. from Tokyo Institute of Technology in 1987. Between 1988 and 1997 he worked as Assistant Professor, Lecturer, and then Associate Professor at Chiba University, 1997–1999 as Associate Professor at the Institute for Molecular Science (IMS) in Okazaki, and 1999–2002 as Full Professor at Nagoya University. In 2002 he became a Full Professor at The University of Tokyo. He has been a leader of the CREST (Core Research for Evolutional Science and Technology) project of the Japan Science and Technology Corporation (JST) since 1998. His research interests include metal-assembled complexes, molecular recognition, and nanometer-sized molecules.